Table 3. Number of anomalous $ALICE_{NDSI}$ pixels detected in the 4-8 December 2013 period, included or not within the PAI area all over the scene and only for the white box (Figure 12b).

	All scene		Black Box	
	Pixels Number	**%**	**Pixels Number**	**%**
included in PAI area	617	68%	537	76%
not included in PAI area	295	32%	172	24%

The analysis of the results reveals that 68% of detected pixels within the whole ROI were in agreement with the PAI area. In addition, looking at Figure 12a, only a very low number of pixels seem to not be directly correlated with the hydrographic network of the ROI, indicating a general good reliability of the achieved results. In more detail, among the 32% of detections outside PAI area (equal to 295 pixels), i) 20% (i.e., 60 pixels) is related with the area/border of the two already cited dams, ii) 36% (i.e., 105 pixels) takes into account of pixels close to the coastline as well as to the rivers but outside the above mentioned zone and hence likely to be considered false positives, iii) the most of the remaining 44% (i.e., 130 pixels) of pixels is clustered in two sub-areas, clearly visible in Figure 12b, one is located between the mouth of the Bradano and Basento rivers and the other is on the left side of the Lato River. The first one was already identified as inundated by Reference [31] and [37], the latter, here identified for the first time, refers to the Castellaneta Marina village, where the freeway "StradaStatale 106" was closed due to the large presence of water [32–36]. Furthermore, it is worth mentioning that these two areas with an estimated extension of about 18.3 km^2, are not contemplated in the current flood risk map, suggesting a potential of satellite-based products even in terms of assessing (and possibly refining) such administrative instruments.

The performance of the results improves when considering only the area within the black box, namely that mainly affected by the event. In particular, among the 172 pixels not included in the PAI area, 31 (i.e., 18%) are probably due to spurious effects, while the remaining 141 pixels (i.e., 82%) correspond to above-mentioned "flooded for sure" areas. Finally, 96% of the detected anomalies within the black box can be considered as real flooded area. This number decreases (i.e., 82%) accounting for the whole ROI, even if 36%, of the remaining 18%, is related with the borders of the San Giuliano and Monte Cotugno dams. Therefore, in absence of other information/documentation about other inundated zones within the ROI, only a residual possible 18% of false positives has been estimated, mostly related to the 7 December image. This achievement confirms the $ALICE_{NDSI}$ capability in flooded area detection with a high level of reliability.

4.3.3. Comparison with VNG

The VNG maps generated for the analysed VIIRS data are plotted in Figure 5, where pixels with an increasing percentage of floodwater fractions are depicted from cyan to red. In these maps it is possible to identify different and quite persistent flooded area, mostly located along the Basento and Lato rivers as well as at the border of the Monte Cotugno and San Giuliano dams. Finally, the north-eastern sector of Figure 5a,b,d is characterized by some possible false positives, probably related to cloud shadows.

All these features are also evident in Figure 13, where flooded pixels, detected by means the $ALICE_{NDSI}$ implementation (red pixels), have been superimposed on those identified by VNG (yellow pixels), regardless their confidence level. Pixels commonly identified as flooded by both the algorithms have been depicted in green.

The two products generally show a good agreement, considering that both the algorithms are able to detect the main spatial features along the Basento and Lato rivers as well as the areas bordering the Monte Cotugno and San Giuliano dams. Even taking into account a different sensitivity in the identification of probably flooded pixels, residual biases are due to effects related to the different land-sea mask used as well as to the already mentioned cloud shadows issues. Table 4 summarizes the

number of probably flooded pixels detected by RST-FLOOD and VNG considering both the whole scene as well as the black box for the five analysed days, exploring also common detections.

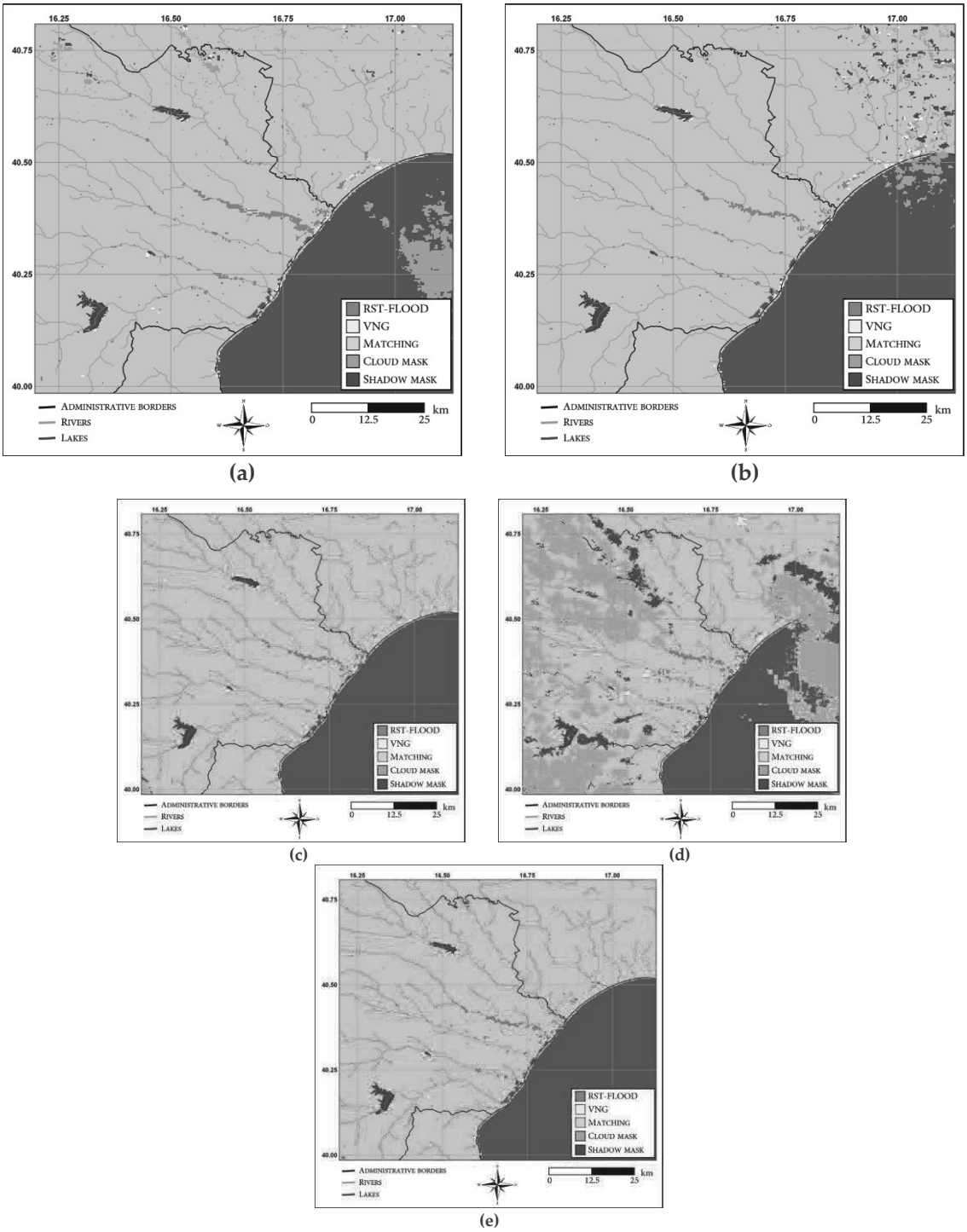

Figure 13. Comparison between flooded areas detected by RST-FLOOD using $\text{ALICE}_{\text{NDSI}} \geq 3$ (red pixels) and VNG (yellow pixels) on VIIRS data acquired on: (**a**) 04/12/2013; (**b**) 05/12/2013; (**c**) 06/12/2013; (**d**) 07/12/2013; (**e**) 08/12/2013. Common detections are depicted in green.

Table 4. Number of pixels detected by RST-FLOOD, VNG and by both the algorithms (as shown in Figure 13) for the analysed days.

	All Scene Pixels Number			Black Box Pixels Number		
VIIRS Data	**RST-FLOOD**	**VNG**	**MATCHING**	**RST-FLOOD**	**VNG**	**MATCHING**
04/12/2013	638	454	109	510	184	96
05/12/2013	357	481	36	293	111	31
06/12/2013	267	234	26	226	84	18
07/12/2013	345	196	4	317	71	4
08/12/2013	260	137	3	211	10	0

VNG seems to detect fewer anomalous pixels than RST-FLOOD, especially along the Basento River, as is clearly observable in Figure 13. This effect is more evident considering the detection statistics related to the black box, where the area most affected by the event is included. The comparison between VNG results and those achieved by the change detection scheme on Landsat data, as already done for RST in Section 4.3.1, returns a 26% of common detections (i.e., 49 pixels) on the whole scene and a 47% in the black box. Starting from the 6 December 2013 (Figure 13c) map, any flooded area around the Basento River has been detected by VNG, whose identifications are mainly focused on Lato River. It is worth noting that, to reduce the false detection [11], the minor flood detection within VNG is only done around the determined floodwater pixels or existing normal water pixels (rivers, lakes or reservoirs) and therefore a water mask not perfectly updated could be at the basis of these discrepancies.

5. Discussion

Floods are natural disasters that, due to their clear spatial and spectral markers in different regions of the electromagnetic spectrum, are more easily investigable by means of satellite data [14]. Among the different satellite-based contributions useful for the flood risk management cycle, is the generation of reliable multi-temporal flood maps is fundamental in all the different phases [8,60,61]. Optical sensors onboard polar satellites can assure the better trade-off among spectral/spatial/temporal resolutions suitable for a near real time and continuous monitoring of flooded area [62] although cloud coverage can fully or partially hamper the acquisition of useful data in this spectral region, possibly limiting their applicability [7]. Among the currently operational optical sensors, VIIRS onboard SNPP is one of the most recent and advanced, assuring a long-term continuity of observation (up to the 2031, [38,39]), that is crucial to assess its potential in investigating floods as well as other natural disasters [40,54].

In this work, the RST-FLOOD approach, previously applied to AVHRR and MODIS VNIR data, has been fully implemented for the first time on historical series of VIIRS Imagery records for evaluating its capability in detecting inundated area. The adoption of dynamic and local-scale self-adaptive thresholds and the fully independence on any kind of auxiliary/ancillary information are the main RST-FLOOD advantages with respect to traditional techniques [14,23]. Fixed thresholding schemes or ancillary dataset are indeed often used for flooded area detection applications [11,54] as well as for facing issues related to cloud and terrain shadows, representing the main challenges for a fully reliable flood detection [11,54]. The results performance of inundated area identification can indeed largely change depending both on the availability and the accuracy of the used auxiliary/ancillary information [22]. In addition, specific site/local-setting of the investigated scene, as well as seasonal/meteorological variations of the studied signals, may negatively affect the sensitivity of fixed thresholds schemes [14,22].

Focusing on the RST-FLOOD-based application shown in this paper, the flood event that affected the Basilicata and Puglia regions in the first week of December 2013 has been investigated, producing satisfactory results, which further confirm the great potential of the proposed approach in detecting flooded areas.

Flood evolution in the spatiotemporal domain has been accurately identified, well over the spatial extent and temporal interval suggested by other works [31,37]. A total area of about 73 km^2 was

identified as inundated during the investigated period, with a good level of reliability, as highlighted by the validation analysis performed through the comparison with the PAI map. About 68% of the detected anomalies falls within the PAI, 6.5% refers to the borders of the San Giuliano and Monte Cotugno dams, 11.5% takes into account pixels close to the coastlines and rivers but outside the above mentioned zone, representing possible false positives. The remaining 14% represents a "for sure" flooded area located in correspondence of the Castellaneta Marina town and between the Bradano and Basento mouths. This last finding is particularly significant because it highlights an area that, although clearly flooded in 2013, has not yet included in the current flood hazard map, revealing the added value that robust satellite algorithms may provide in improving flood risk management.

Comparison with the results provided by implementing another VIIRS-based method [11] seems to confirm the good capability of RST-FLOOD to detect inundated area. Although some differences are inherently due to the different approach at the basis of the two algorithms, some others are attributable to the assumption that VNG has been developed to work at global scale (between 80 °S and 80 °N) and set more towards reliability than sensitivity. Moreover, a few of the static ancillary databases used within this software might not be updated respect to the local conditions faced in this work.

Despite these satisfactory achievements, a few possible sources of inaccuracies (i.e., the above cited 11.5% of possible false positives) have been identified and are briefly discussed as follows.

Cloud shadows, representing the main issue limiting flood detection reliability, can be considered as random and spurious signals perturbing the reflectance field measured in the VIS-SWIR spectral region. Therefore, in this paper, their identification has been addressed developing an original RST-based approach exploiting VIIRS I1, I2 and I3 bands reflectance (see Section 3.4). In detail, the combination of the signal acquired in these three bands has been used to discriminate cloud shadows from flooded area and other features. Preliminarily results here presented seem to confirm the feasibility of this approach, even if, a few omission errors have been identified, producing false positive detections. Further analyses aimed at assessing the accuracy of these achievements will be performed in the future, in order to better investigate if other possible signal combinations may provide any improvement.

Residual geo-location errors or the use of a land-sea mask not perfectly co-located with the analysed data may produce a few false positive along coastlines. In these zones, the concurrent presence of water and land produces a mixed spectral signature at pixel level that is generally taken into account by standard deviation in the RST-FLOOD approach. When a seawater-like signal is compared with a land-like one a few errors may be detected, thus suggesting a check on the geo-location data accuracy.

The inflow of anomalous concentration of suspended sediments from lakes (dams) within the ROI has affected the signal measured by VIIRS especially at low wavelengths (i.e., I1 band) especially on the RED and SWIR bands combination (i.e., Ratio and Difference), also in terms of ALICE index implementation (see Section 4.1). Within the RST framework, this is an expected and obvious result because it highlights the occurrence of conditions extremely different from the expected one, in terms of RED reflectance variation. On the other hand, within the RST-FLOOD application, the identification of anomalous "flooded" pixels on the lake border could represent for sure a limitation. The NDSI signal is inherently affected by the increase in the RED signal due to suspended sediments but its implementation within RST did not generate evident signal anomalies, thus indicating that the adoption of the normalized signal coupled with the differential approach enables to face any possible issue.

A possible further limitation that could influence the NDSI signal is the presence of snow, which would produce a spectral signature similar to the flooded areas [7] due to the spectral position of VIIRS I3 band (i.e., 1.58–1.64 μm). Concerning this issue, at least two possible scenarios can be defined in the RST context, depending on whether the investigated area is characterized by the presence/absence of permanent snow. The RST local (at pixel scale) differential approach allows at overcoming this limitation for the permanent snow-covered areas that, showing all the time very high NDSI value, will not produce any anomalous ALICE values, also in presence of fresh snow. On the other hand, different